IEEE Access
Multidisciplinary ⋮ Rapid Review ⋮ Open Access Journal

Received October 6, 2021, accepted November 13, 2021, date of publication November 18, 2021,
date of current version November 30, 2021.

Digital Object Identifier 10.1109/ACCESS.2021.3129249

Circuit Configurable Bidirectional DC-DC Converter for Retired Batteries

JENHAO TENG, (Senior Member, IEEE), POSHENG SHEN, BOHSIEN LIU, AND SIWEI CHEN
Department of Electrical Engineering, National Sun Yat-sen University, Kaohsiung 80424, Taiwan

Corresponding author: Jenhao Teng (jhteng@ee.nsysu.edu.tw)

This work was supported in part by the Ministry of Science and Technology of Taiwan under Contract MOST 108–2221-E-110–041-MY3 and Contract MOST 108–2622–E–110–007-CC2.

ABSTRACT Due to the rapid development and widespread usage of Electric Vehicles (EVs), there will be more and more retired batteries in the future. These retired batteries can be used in energy storage systems to stabilize smart grid operation with high penetration of renewable energy. The battery modules used in EVs are equipped with dedicated bidirectional converters. However, if a dedicated bidirectional converter is required for a retired battery, it will cause resource waste and increase the difficulty of reuse. Therefore, it is vital to design and develop a bidirectional DC-DC converter with a wide-range voltage conversion ratio due to the various voltage levels of retired batteries. Especially, the designed converter should have the bidirectional voltage boost and buck abilities to change the different voltage levels of retired batteries for different application scenarios. A circuit configurable bidirectional DC-DC converter for retired batteries is proposed in this paper. The proposed converter is constituted by cascading a two-phase interleaved half-bridge circuit and a voltage-doubler circuit and can be operated in the interleaved boost/buck mode, single boost/buck mode, cascaded-buck-boost mode, or single buck/boost mode concerning the voltage levels at the terminals of the proposed converter. Due to the circuit configurable design of the proposed converter, a wide-range voltage conversion ratio and bidirectional buck and boost abilities can be achieved. A prototype circuit for the proposed bidirectional DC-DC converter with a rated voltage of 150V at the terminal of two-phase interleaved half-bridge circuit, a rated voltage between 25V and 1050V at the terminal of voltage-doubler circuit, and a rated power of 1100W is designed and implemented. Experimental results show that the proposed converter can be configured into the diverse operating modes for different voltage levels and above 98% of the maximum conversion efficiency can be realized.

INDEX TERMS Electric vehicle, bidirectional DC-DC converter, retired battery, circuit configurable, two-phase interleaved half-bridge circuit, voltage-doubler circuit.

I. INTRODUCTION

Bidirectional DC-DC converters can be effectively interfaced between power sources and energy storages to reduce the size and enhance the efficiency of the conventional two individual converters used for the forward and reverse power flow [1]. Bidirectional DC-DC converters have been widely employed in different applications including uninterruptible power supplies, Electric Vehicles (EVs), Energy Storage Systems (ESSs), renewable energy systems, and so on [1]–[7]. The topologies, control schemes, and applications of bidirectional DC–DC converters were discussed and investigated in [1], [2]. The PV-battery-based bidirectional DC-DC converter for household applications was proposed in [3]. Refs. [4], [5] reviewed the non-isolated bidirectional DC-DC converters for ESSs and Plug-in Hybrid EVs (PHEVs). Refs. [6], [7] investigated the high-power-quality grid interface and applications of DC-microgrid grid using the bidirectional DC-DC converters of EVs. Besides, with the global trend of carbon emission reduction and energy saving, many countries have treated electrified vehicles, including EVs and PHEVs, as one of the most important measures for greenhouse gas reduction. The global EV market was valued at $162.34 billion in 2019 is predicted to have $802.81 billion by 2027 at a compound annual growth rate of 22.6% [8]. The charging performance of EVs has a decisive influence on the development of EVs. Therefore, bidirectional DC-DC converters with lower cost, higher conversion efficiency,

The associate editor coordinating the review of this manuscript and approving it for publication was Zhiyi Li.

and higher operational reliability are essential for EV charging.

EV's batteries can be treated as ESSs to absorb the grid power to the EV's batteries during the off-peak-load period and to supply power from EV's batteries to the grid in the peak-load period. This functionality is regarded as a Vehicle to Grid (V2G) application. The bidirectional DC-DC converters can also be used in EVs or PHEVs with V2G functionality to charge the batteries from the grid and to discharge the energy stored in EVs' or PHEVs' batteries to the grid depending on grid requests. In addition, when the state of health of EV's batteries drops to 80%, the batteries are no longer suitable for on-road usage and will be retired [9], [10]. The retired batteries can still be used in ESSs to help stabilize the renewable energy systems and reduce household electricity consumption. Due to the rapid development and widespread use of EVs, it is foreseeable that there will be more and more retired batteries in the future [9]–[12]. The battery modules used in EVs are equipped with dedicated bidirectional converters; however, if a dedicated bidirectional converter is required for a retired battery, it will cause resource waste and increase the difficulty of reuse. The voltage ranges of retired batteries obtained from different EVs, such as electric scooters, electric cars, electric buses, electric trucks, etc., are shown in Figure 1 [12]. It can be observed that the voltages of retired batteries may commonly vary from 24V to 800V; therefore, a bidirectional DC-DC converter with a wide-range voltage conversion ratio will play an important role in the reuse of retired batteries.

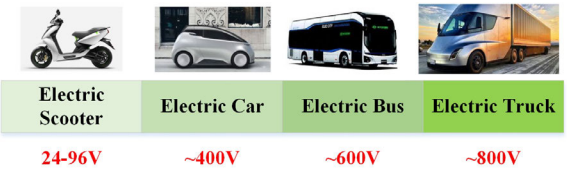

FIGURE 1. Voltage level ranges of different EVs.

The bidirectional DC-DC converters can be classified into isolated and non-isolated circuit topologies. The non-isolated circuit topologies transfer the power without the magnetic isolation of a transformer; therefore, the magnetic interference and heavier weight of the transformer can be avoided making them suitable for the limited size and weight applications. The isolated topologies need a high-frequency transformer to transmit power; therefore, the advantages of galvanic isolation and a higher voltage gain ratio can be obtained. However, the transformer should be carefully designed to prevent the leakage inductance effect and magnetic interference. Most of the non-isolated circuit topologies are designed based on the conventional DC-DC converters such as buck, boost, buck-boost, Cuk, etc. combining with voltage boosting, switched capacitor, interleaved, and multilevel techniques [13]–[20]. The fundamental non-isolated bidirectional DC-DC converters include buck- and boost-based bidirectional converter [13], buck-boost-based bidirectional converter [14], Cuk-based bidirectional converter [15], Single-Ended Primary-Inductor Converter (SEPIC) and Zeta-based bidirectional converter [16], cascaded bidirectional converter [17], switched-capacitor-based bidirectional converter [18], interleaved/multilevel bidirectional converter [19], [20] etc. Among those topologies, the cascaded bidirectional converter [17] was designed to be used in EV applications with low-loss, constant-frequency, and zero-voltage-switching features. The switched-capacitor-based bidirectional converter [18] was realized by the improvement of a unidirectional switched-capacitor-based converter. There was no inductor in its original design and therefore the advantages are lower size and weight and the main disadvantage is the current continuity. The interleaved/multilevel bidirectional converter [19], [20], used the interleaving technique to reduce the current ripple and filter size, and the multilevel technique to obtain a higher voltage gain, was designed for higher power/voltage applications.

The fundamental isolated bidirectional DC-DC converters include flyback-based bidirectional converter [21], Cuk, SEPIC and Zeta-based bidirectional converter [22], [23], push-pull-based bidirectional converter [24], forward bidirectional converter [25], dual-active-bridge-based bidirectional converter [26], dual-active-half-bridge-based bidirectional converter [27], multiport bidirectional converter [28] etc. Among those topologies, back-to-back bidirectional topologies using voltage-fed or current-fed, half-bridge or full-bridge configurations isolated by a transformer are the most commonly-used isolated bidirectional DC-DC converters. The dual-active-bridge-based bidirectional converter [26] used eight power switches along with an isolated transformer made it have a high voltage gain ratio and was suitable for high power applications. Comparing with a full-bridge configuration, the number of power switches in a half-bridge configuration is reduced to four and can be usually used in lower power applications. Based on these circuit topologies [13]–[28], many new bidirectional converters with wide voltage conversion ranges have been developed and part of them suitable for EVs are discussed [29]–[33]. A transformerless bidirectional DC-DC converter with wide conversion ratios was proposed in [29]. Ref. [30] combined a three-phase interleaved structure with switched-capacitor cells to construct a switched-capacitor interleaved bidirectional DC-DC converter. Adjusting the inductance of inductors in [29] and [30] can achieve a wide-range voltage conversion ratio; however, it may cause additional leakage inductance problems. A bidirectional DC-DC converter using the modified nondissipative current snubber in a SEPIC converter was proposed in [31]. The conversion efficiency and conversion voltage ratio might be limited by the duty cycles of the switches. The new bidirectional dc-dc converters with high voltage conversion ratios were presented in [32], [33]. The voltage conversion ratio is high; however, the voltage range is restricted and may require more switches and capacitors.

In general, the conventional non-isolated and isolated bidirectional DC-DC converters act as a buck or boost mode and the controller regulates the voltage or current of the converters according to the voltages of energy storage. Most of these converters cannot achieve bidirectional voltage boost and buck abilities; therefore, they might not be suitable for the various voltage conversions of retired batteries. For example, a bidirectional DC-DC converter with buck and boost modes for charging and discharging, respectively is required for the retired batteries obtained from electric scooters with voltages about 24V to 96V. On the contrary, a bidirectional DC-DC converter with boost and buck modes for charging and discharging, respectively is commonly needed for the retired batteries obtained from electric trucks with voltages about 600V to 800V. Therefore, a novel bidirectional DC-DC converter for retired batteries should have the bidirectional voltage boost and buck abilities to change the different voltage levels of retired batteries for different application scenarios. A circuit configurable bidirectional DC-DC converter for retired batteries is proposed in this paper. The proposed converter is constituted by cascading a two-phase interleaved half-bridge circuit and a voltage-doubler circuit. The proposed converter can be operated in the interleaved boost/buck mode, single boost/buck mode, cascaded-buck-boost mode, or single buck/boost mode concerning the voltage levels at different terminals of the proposed converter. Due to the configurable structure design and control of the proposed converter, a wide-range voltage conversion ratio and bidirectional buck and boost abilities can be achieved. Therefore, the proposed converter can be utilized in the energy conversion of different retired batteries, such as electric scooters, EVs, electrical buses, electric trucks, and so on. A prototype circuit for the proposed bidirectional DC-DC converter with a rated voltage of 150V at the terminal of two-phase interleaved half-bridge circuit, a rated voltage between 25V and 1050V at the terminal of voltage-doubler circuit, and a rated power of 1100W is designed and realized. Experimental results show that the proposed converter can be configured into the different operating modes for different voltage levels and above 98% of the maximum conversion efficiency can be realized. Experimental results also demonstrate that the proposed circuit configurable converter can be used for the diverse voltage level conversions of retired batteries.

II. CIRCUIT TOPOLOGY OF PROPOSED CONVERTER

Figure 2 shows an interleaved DC-DC converter with a high buck conversion ratio proposed in [34], [35]. It can be seen that the circuit consists of two inductors, four power switches, two diodes, four input capacitors, and one output capacitor. Among them, the four capacitors are used for energy storage and voltage division, which can reduce the voltage stress on the power switches and increase the buck conversion ratio. The ripple inductor currents can be reduced by 50% with interleaving operation. A bidirectional DC-DC converter might be realized if the diodes in Figure 2 are changed to power switches. Although the circuit configuration of Figure 2 has a higher buck voltage conversion ratio, it cannot achieve bidirectional buck and boost abilities. Figure 3 shows a bidirectional, cascaded, and buck-boost DC-DC converter used in EVs or fuel cell vehicles [17]. The characteristic of Figure 3 is that the energy can be elastically transferred. It improves the traditional DC-DC converter that can only be used in the one-way buck-boost application. This architecture can buck and boost conversions in any direction; however, it has a relatively lower voltage conversion ratio. To improve those problems, a bidirectional DC-DC converter with a wide-range conversion ratio and bidirectional buck and boost abilities is proposed in this paper.

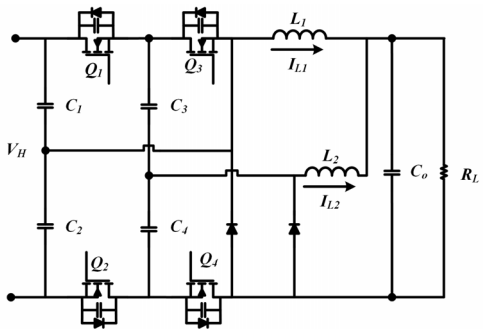

FIGURE 2. DC-DC converter with a high buck conversion ratio.

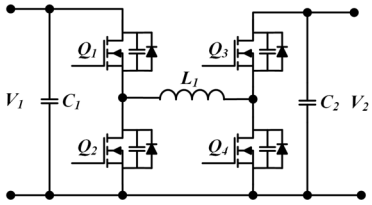

FIGURE 3. DC-DC converter with a bidirectional buck and boost modes.

Ref. [36] represented a bidirectional DC-DC converter with a wide-range voltage conversion ratio. The basic concepts of the converter proposed in this paper were developed; however, the detailed operational modes, comparisons with the conventional bidirectional converters, and experimental results were not discussed in [36] and are investigated in this paper. The proposed circuit configurable bidirectional DC-DC converter is constituted by cascading a two-phase interleaved half-bridge circuit and a voltage-doubler circuit. With the proposed converter, the bidirectional voltage boost and buck abilities can be achieved and therefore can be used for the various voltage level conversions of retired batteries. Figure 4 shows the circuit topology of the proposed bidirectional DC-DC converter. For simplification, the terminals of two-phase interleaved half-bridge circuit and voltage-doubler circuit are denoted as **TIHB** and **TVD**, respectively. The proposed converter can be operated in the interleaved-boost mode, single-boost mode, cascaded-buck-boost mode, or single-buck mode for the power transmitted from TIHB to TVD. On the contrary, for the power converted from TVD and TIHB the proposed converter can be

operated in the interleaved-buck mode, single-buck mode, cascaded-buck-boost mode, or single-boost mode. The basic circuit topology of the proposed converter is composed of a two-phase interleaved half-bridge circuit and a voltage-doubler circuit. Although the basic circuits of the proposed converter existed, a wide-range voltage conversion ratio and bidirectional buck and boost abilities can be achieved due to the configurable structure and control proposed in this paper. Therefore, the proposed converter can be utilized in the energy conversion of different retired batteries. The detailed operating stages of each mode will be discussed in the next section.

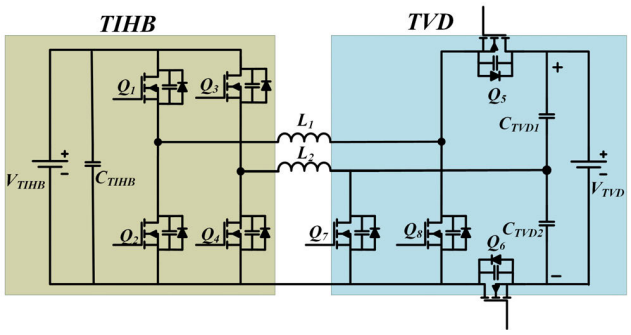

FIGURE 4. Circuit topology of the proposed bidirectional converter.

III. OPERATIONAL MODES OF PROPOSED CONVERTER

A. OPERATIONAL MODES FROM TIHB TO TVD

When the power is transmitted from TIHB to TVD, the voltages at TIHB and TVD are defined as the input voltage and output voltage, respectively. Figure 5 shows the configured circuit topologies of the proposed converter operated in the interleaved-boost mode, single-boost mode, cascaded-buck-boost mode, and single-buck mode concerning the voltage levels of TVD, respectively.

The switch operation states of each mode are listed in TABLE 1. For the interleaved-boost mode, the signals of switches Q_1 and Q_3 are normally ON; the signals of switches Q_2 and Q_4 are normally OFF; and the PWMs of switches Q_5 and Q_8 and the PWMs of switches Q_6 and Q_7 are complementary, respectively. Besides, the PWM phases of switches Q_6 and Q_7 are shifted by 180 degrees. For the single-boost mode, the signals of switches Q_1 and Q_6 are normally ON; the signals of switches Q_2, Q_3, Q_4, and Q_7 are normally OFF; and the PWMs of switches Q_5 and Q_8 are complementary. For the cascaded-buck-boost mode, the signal of switch Q_6 is normally ON; the signals of switches Q_3, Q_4, and Q_7 are normally OFF; and the PWMs of switches Q_1 and Q_2 and the PWMs of switches Q_4 and Q_5 are complementary, respectively. For the single-buck mode, the signals of switches Q_5 and Q_6 are normally ON; the signals of switches Q_3, Q_4, Q_7, and Q_8 are normally OFF; and the PWMs of switches Q_1 and Q_2 are complementary. Only the operational stages of the interleaved-boost mode from TIHB to TVD are discussed here due to limited space.

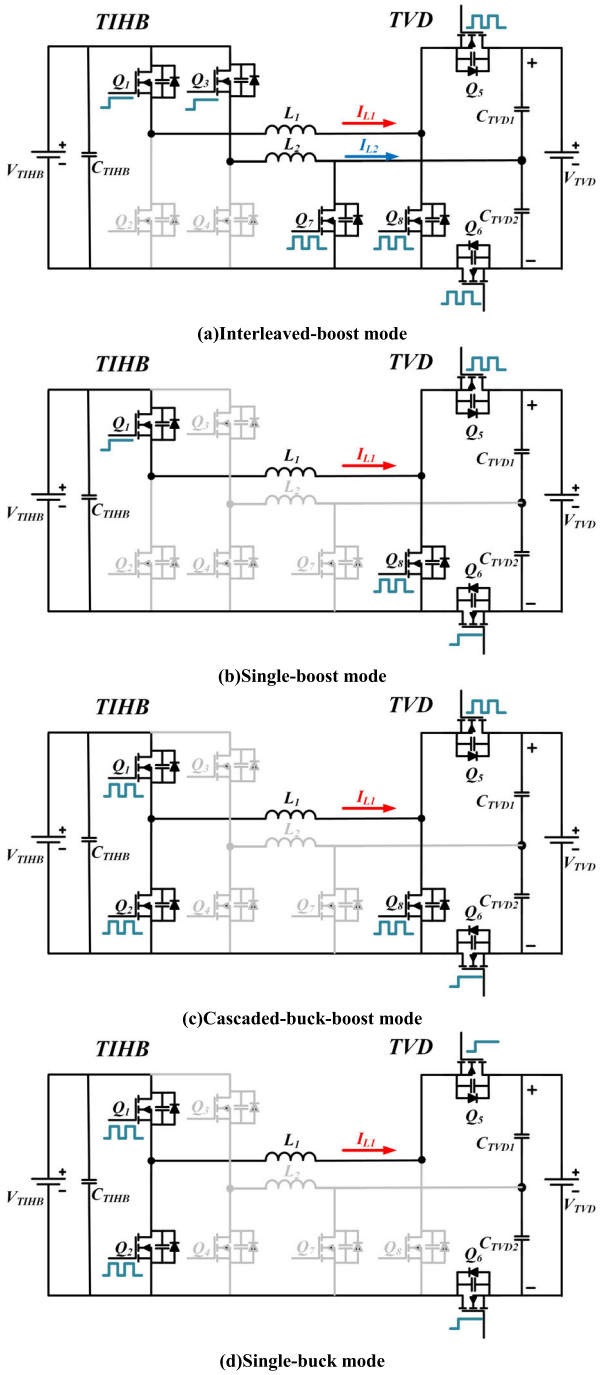

FIGURE 5. Operational circuit topologies for the proposed converter from TIHB to TVD.

The theoretical waveforms of the interleaved-boost mode from TIHB to TVD operated at 75% of the duty cycles for switches Q_7 and Q_8 are shown in Figure 6. The signals of switches Q_1 and Q_3 and the signals of switches Q_2 and Q_4 are normally ON and normally OFF, respectively; thus, their signal waveforms are not shown. As illustrated in Figure 6, V_{dsi} is the drain-source voltage of switch Q_i; V_{gsi} is the drive signal of switch Q_i; and i_{L1} and i_{L2} are the currents of inductors L_1 and L_2, respectively. According to the time

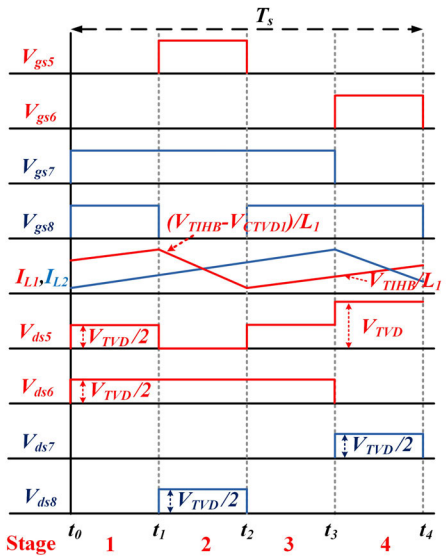

FIGURE 6. Theoretic waveforms of interleaved-boost mode from TIHB to TVD.

interval of the theoretical waveforms illustrated in Figure 6, the following four operational stages as illustrated in Figure 7 are determined.

Stage 1 [t_0, t_1] of interleaved-boost mode: As illustrated in Figure 7(a), the PWMs of switches Q_7 and Q_8 are in the ON state and the PWMs of the switches Q_5 and Q_6 are in the OFF state. The cross voltages at the inductors L_1 and L_2 are both V_{TIHB}. The inductor currents i_{L1} and i_{L2} rise linearly and the energy is stored in the inductors L_1 and L_2. Meanwhile, the energy stored in the capacitors C_{TVD1} and C_{TVD2} is released to TVD (V_{TVD}) together.

Stage 2 [t_1, t_2] of interleaved-boost mode: At t_1, the PWMs of switches Q_5 and Q_8 change to the ON and OFF states, respectively. Figure 7(b) indicates that PWMs of the switches Q_5 and Q_7 are in the ON state and the PWMs of switches Q_6 and Q_8 are in the OFF state. The cross voltage of the inductor L_1 is (V_{TIHB}–V_{CTVD1}). Comparing to Stage 1, the inductor current i_{L1} declines linearly, and the energy stored in the inductor L_1 is transferred to the capacitor C_{TVD1}. The cross voltage of the inductor L_2 is V_{TIHB} and the inductor current i_{L2} still rises linearly.

Stage 3 [t_2, t_3] of interleaved-boost mode: At t_2, the PWMs of switches Q_5 and Q_8 change to the OFF and ON states, respectively. The PWMs of switches Q_7 and Q_8 are in the ON state and the PWMs of switches Q_5 and Q_6 are in the OFF state; therefore, this stage is the same as described in stage 1 and is shown in Figure 7(c).

Stage 4 [t_3, t_4] of interleaved-boost mode: At t_3, the PWMs of switches Q_6 and Q_7 change to the ON and OFF states, respectively. As shown in Figure 7(d), the PWMs of switches Q_6 and Q_8 are in the ON state and the PWMs of switches Q_5 and Q_7 are in the OFF state. The cross voltage of the inductor L_2 is (V_{TIHB}–V_{CTVD2}). The inductor current i_{L2} declines linearly and the energy stored in the inductor L_2 is transferred to the capacitor C_{TVD2}. The cross voltage of the inductor L_1 is V_{TIHB} and the inductor current i_{L1} rises linearly.

As shown in Figures 6 and 7, the average voltages of inductors L_1 and L_2 can be calculated from the operational stages 1 to 4 of interleaved boost mode and be written as

$$V_{L1} = \frac{1}{T_S}(V_{TIHB}(t_1 - t_0) + (V_{TIHB} - V_{CTVD1})(t_2 - t_1) + V_{TIHB}(t_3 - t_2) + V_{TIHB}(t_4 - t_3)) \quad (1a)$$

$$V_{L2} = \frac{1}{T_S}(V_{TIHB}(t_1 - t_0) + V_{TIHB}(t_2 - t_1) + V_{TIHB}(t_3 - t_2) + (V_{TIHB} - V_{CTVD2})(t_4 - t_3)) \quad (1b)$$

The average current at TIHB can be expressed as

$$I_{TIHB} = I_{L1} + I_{L2} \quad (2)$$

where T_S is the switching cycle time. V_{TIHB} and I_{TIHB} are the average voltage and current of TIHB. V_{CTVD1} and V_{CTVD2} are the average voltages of output capacitors C_{TVD1} and C_{TVD2}, respectively. V_{L1} and V_{L2} are the average voltages of inductors L_1 and L_2, respectively. I_{L1} and I_{L2} are the average currents of inductors L_1 and L_2, respectively.

Using the volt-second balance, the following formulas can be derived

$$V_{L1} = V_{TIHB} - V_{CTVD1}D_{Q8} = 0 \quad (3a)$$

$$V_{L2} = V_{TIHB} - V_{CTVD2}D_{Q7} = 0 \quad (3b)$$

where D_{Q5} and D_{Q6} are the duty cycles of switches Q_5 and Q_6, respectively. Generally, L_1 is equal to L_2 and C_{TVD1} is equal to C_{TVD2}, the average voltage of TVD and voltage

TABLE 1. Switch operation states of each mode from TIHB to TVD.

Operation Mode	Switch Operation States							
	Q_1	Q_2	Q_3	Q_4	Q_5	Q_6	Q_7	Q_8
Interleaved Boost	**Normally ON**	**Normally OFF**	**Normally ON**	**Normally OFF**	PWM-Q_5	PWM-Q_6	PWM-Q_7	PWM-Q_8
Single Boost	**Normally ON**	**Normally OFF**	**Normally OFF**	**Normally OFF**	PWM-Q_5	**Normally ON**	**Normally OFF**	PWM-Q_8
Cascaded Buck-Boost	PWM-Q_1	PWM-Q_2	**Normally OFF**	**Normally OFF**	PWM-Q_5	**Normally ON**	**Normally OFF**	PWM-Q_8
Single Buck	PWM-Q_1	PWM-Q_2	**Normally OFF**	**Normally OFF**	**Normally ON**	**Normally ON**	**Normally OFF**	**Normally OFF**

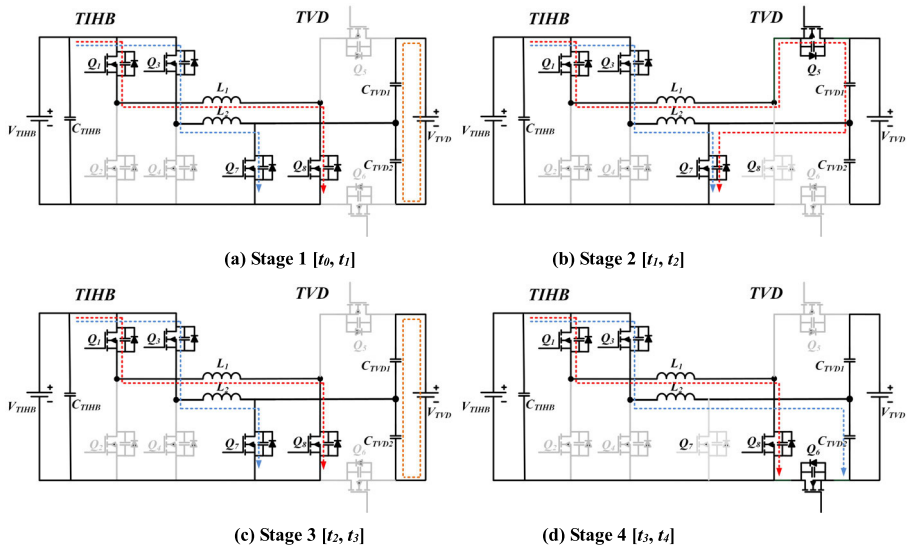

FIGURE 7. Operational stages of interleaved boost mode from TIHB to TVD.

conversion ratio can then be calculated by

$$V_{TVD} = V_{CTVD1} + V_{CTVD2} \tag{4a}$$

$$\frac{V_{TVD}}{V_{TIHB}} = \frac{2}{1 - D_{Q7}} = \frac{2}{1 - D_{Q8}} \tag{4b}$$

where D_{Q7} and D_{Q8} are the duty cycles of switches Q_7 and Q_8, respectively. Note that the PWMs of switches Q_5 and Q_8 and the PWMs of switches Q_6 and Q_7 are complementary, respectively.

TABLE 2 shows the voltage conversion ratio, the number of switches operated by PWM signals, normally ON and normally OFF of each mode for the power transmitted from TIHB to TVD. When the voltage at TIHB is fixed, the 8-times and 4-times boost voltage conversion ratios can be approximately obtained by the interleaved-boost mode and single-boost mode with the duty cycle of 75% at switch Q_8, respectively. The different ranges of boost voltage conversion ratio can be realized while the duty cycles are adjusted. The voltage conversion ratio of cascaded-buck-boost mode can be controlled by adjusting the duty cycles of the switches Q_1 and Q_5. The cascaded-buck-boost mode is recommended to be used when the voltage levels of TIHB and TVD are close. The single-buck mode is used when the voltage at TIHB is higher than the voltage at TVD. The 4-times buck voltage conversion ratio can be achieved with the duty cycle of 25% at switch Q_1.

B. OPERATIONAL MODES FROM TVD TO TIHB

The voltages at TVD and TIHB are denoted as the input voltage and output voltage, respectively. The power transmitted from TVD to TIHB can be considered as the reverse operations of modes from TIHB to TVD as illustrated in Figure 5; therefore, the proposed converter can be operated in the interleaved-buck mode, single-buck mode, cascaded-buck-boost mode, and single-boost mode for the voltage levels of TIHB. The circuit topologies are the same as shown in Figure 5(a)-Figure 5(d), respectively; however, the currents flow from TVD to TIHB. The switch operation states of each mode are the same as listed in TABLE 1. For example, the signal of switch Q_6 is normally ON; the signals of switches Q_3, Q_4, and Q_7 are normally OFF; the PWMs of switches Q_1 and Q_2 and the PWMs of switches Q_4 and Q_5 are complementary, respectively for the cascaded-buck-boost mode. The theoretical waveforms of the cascaded-buck-boost mode from TVD to TIHB operated at 50% of the duty cycles for Q_1 and Q_5 are shown in Figure 8. The signals of switches Q_3, Q_4, and Q_7 and the signal of switch Q_6 are normally OFF and normally ON, respectively; therefore, their signal waveforms are not shown. According to the time interval of the theoretical waveforms illustrated in Figure 8, the following four operational stages as illustrated in Figure 9 are determined.

Stage 1 [t_0, t_1] of cascaded-buck-boost mode: As illustrated in Figure 9(a), the PWMs of switches Q_2 and Q_5 are in the ON state and the PWMs of the switches Q_1 and Q_8 are in the OFF state. The cross voltage at the inductors L_1 is V_{TVD}. The inductor current i_{L1} rises linearly and the energy is stored in the inductor L_1. Meanwhile, the energy stored in the capacitor C_{TIHB} is released to TIHB (V_{TIHB}).

Stage 2 [t_1, t_2] of cascaded-buck-boost mode: At t_1, the PWMs of switches Q_1 and Q_2 change to the ON and OFF states, respectively as shown in Figure 8. Figure 9(b) indicates that PWMs of the switches Q_1 and Q_5 are in the ON state and the PWMs of switch Q_2 and Q_8 are in the OFF state. The cross voltage of the inductor L_1 is (V_{TVD}-V_{TIHB}). The inductor current i_{L1} rises linearly if V_{TVD} is larger than V_{TIHB}. On the contrary, the inductor current i_{L1} declines linearly while V_{TVD} is less than V_{TIHB}.

Stage 3 [t_2, t_3] of cascaded-buck-boost mode: At t_2, the PWMs of switches Q_5 and Q_8 change to the OFF and ON

TABLE 2. Characteristics of proposed converter From TIHB to TVD.

Mode	Voltage Conversion Ratio	No. of Switches w. PWM	No of Switches w. Normally ON	No. of Switches w. Normally OFF
Interleaved Boost	$2/(1-D_{Q8})$	4	2	2
Single Boost	$1/(1-D_{Q8})$	2	2	4
Cascaded Buck-Boost	D_{Q1}/D_{Q5}	4	1	3
Single Buck	D_{Q1}	2	2	4

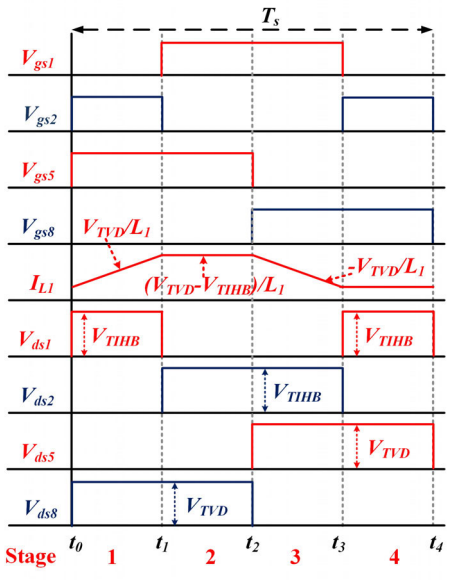

FIGURE 8. Theoretic waveforms of cascaded-buck-boost mode from TVD to TIHB.

states, respectively. The PWMs of switches Q_1 and Q_8 are in the ON state and the PWMs of switches Q_2 and Q_5 are in the OFF state as shown in Figure 9(c). The cross voltage of the inductor L_1 is -V_{TIHB}; therefore, the inductor current i_{L1} declines linearly and the energy stored in the inductor L_1 is transferred to the capacitor C_{TIHD}.

Stage 4 [t_3, t_4] of cascaded-buck-boost mode: At t_3, the PWMs of switches Q_2 and Q_1 change to the ON and OFF states, respectively. As shown in Figure 9(d), the PWMs of switches Q_2 and Q_8 are in the ON state and the PWMs of switches Q_1 and Q_5 are in the OFF state. The cross voltage of the inductor L_1 is 0; therefore, the inductor current i_{L1} remains constant. The energy stored in the capacitor C_{TIHB} is released to TIHB (V_{TIHB}).

According to the operational stages shown in Figures 8 and 9, the average voltage of inductor L_1 can be calculated by

$$V_{L1} = \frac{1}{T_S}(V_{TVD}(t_1 - t_0) + (V_{TVD} - V_{TIHB})(t_2 - t_1) - V_{TIHB}(t_3 - t_2) + 0(t_4 - t_3)) \quad (5)$$

The average current at TVD can be expressed as

$$I_{TVD} = \frac{1}{T_S}(I_{L1}(t_1 - t_0) + I_{L1}(t_2 - t_1) + 0(t_3 - t_2) + 0(t_4 - t_3)) = D_{Q5}I_{L1} \quad (6)$$

Using the volt-second balance, the following formula can be derived

$$V_{L1} = D_{Q5}V_{TVD} - D_{Q1}V_{TIHB} = 0 \quad (7)$$

The voltage conversion ratio can then be calculated by

$$\frac{V_{TIHB}}{V_{TVD}} = \frac{D_{Q5}}{D_{Q1}} \quad (8)$$

Note that the PWMs of switches Q_1 and Q_2 and the PWMs of switches Q_4 and Q_5 are complementary, respectively. If the duty cycle of switch Q_1 is 50%, the boost and buck effects can be achieved while the duty cycle of switch Q_5 is greater and less than 50%, respectively.

TABLE 3 shows the voltage conversion ratio, the number of switches operated by PWM signals, normally ON and normally OFF of each mode for the energy transferred from TVD to TIHB. When the voltage at TVD is fixed, the 8-times and 4-times buck voltage conversion ratios can be obtained by the interleaved-buck mode and single-buck mode with the duty cycle of 25% at switch Q_5, respectively. The voltage conversion ratio of cascaded-buck-boost mode can be controlled by adjusting the duty cycles of the switches Q_1 and Q_5 and is recommended to be used when the voltage levels of TVD and TIHB are close. The single-boost mode is used when the voltage at TIHB is higher than the voltage at TVD. The 4-times boost voltage conversion ratio can be achieved with the duty cycle of 75% at switch Q_1. From the operational modes described above, it can be clearly observed that a wide-range bidirectional boost and buck voltage conversion ratio through the proposed circuit configurable bidirectional DC/DC converter can be realized. Therefore, the proposed converter can be utilized in the energy conversion of different retired batteries.

TABLE 4 lists the comparisons of the proposed converter with the fundamental non-isolated bidirectional converters from the viewpoints of the voltage conversion ratio, number of switches, inductors, capacitors, etc. For simplification, the Left-Hand Side (LHS) and Right-Hand Side (RHS) mean the low voltage and high voltage of the conventional non-isolated bidirectional converter and are the TIHB and TVD of the proposed converter, respectively. From TABLE 4, it can be seen that the 8 switches, 3 capacitors, and 2 inductors are required to construct the proposed circuit configurable converter.

The proposed converter needs more components than some of the fundamental non-isolated bidirectional converters; however, a wider range voltage conversion ratio can be obtained. For example, it can be calculated that the V_{RHS}/V_{LHS} are 4.0, −3.0, 3.0, 2.0, 4.0 and 4.0 for the buck-boost-based bidirectional converter [13], Cuk-based

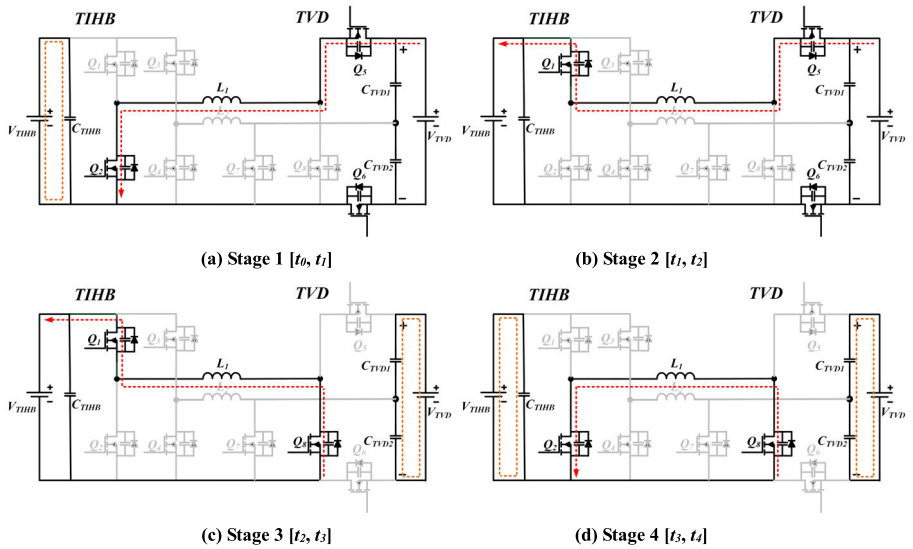

FIGURE 9. Operational stages of cascaded-buck-boost mode from TVD to TIHB.

TABLE 3. Characteristics of proposed converter from TVD to TIHB.

Mode	Voltage Conversion Ratio	No. of Switches w. PWM	No of Switches w. Normally ON	No. of Switches w. Normally OFF
Interleaved Buck	$D_{Q5}/2$	4	2	2
Single Buck	D_{Q5}	2	2	4
Cascaded Buck-Boost	D_{Q5}/D_{Q1}	4	1	3
Single Boost	$1/(1-D_{Q1})$	2	2	4

TABLE 4. Comparisons of proposed converter with the fundamental non-isolated bidirectional converters.

Converter	V_{RHS}/V_{LHS}	No. of Switches	No. of Capacitors	No. of Inductors
Buck-Boost Converter [13]	*1/(1-D)*	2	2	1
Cuk [15]	*-D/(1-D)*	3	3	2
Sepic/Zeta [16]	*D/(1-D)*	2	2	2
Switched Capacitor [18]	*2*	4	3	0
Two-phase Interleaved [19]	*1/(1-D)*	4	2	2
Four-times Multilevel [20]	*4*	20	10	0
Proposed Circuit*	***D~2/(1-D)***	**8**	**3**	**2**

*: The voltage conversion ratio is dependent on the chosen mode

bidirectional converter [15], SEPIC and Zeta-based bidirectional converter [16], Switched-capacitor-based bidirectional converter [18], interleaved bidirectional converter [19] and multilevel bidirectional converter [20], respectively when the duty cycle is 0.75. The V_{RHS}/V_{LHS} of the proposed circuit configurable converter operating in the interleaved-boost mode is 8.0 when the duty cycle is 0.75. When the duty cycle is 0.25, the V_{RHS}/V_{LHS} are 1.33, −0.33, 0.33, 2.0, 1.33 and 1.0 for the buck-boost-based bidirectional converter [13], Cuk-based bidirectional converter [15], SEPIC and Zeta-based bidirectional converter [16], Switched-capacitor-based bidirectional converter [18], interleaved bidirectional converter [19] and multilevel bidirectional converter [20], respectively. At this moment, the V_{RHS}/V_{LHS} of the proposed circuit configurable converter operating in the single-buck mode is 0.25. Obviously, the Cuk-based converter [15], SEPIC, and Zeta-based converter [16] and the proposed converter can realize the boost and buck voltage conversions from V_{RHS} to V_{LHS}. However, the proposed circuit configurable converter can achieve a wider range voltage conversion ratio than other non-isolated conventional converters.

IV. EXPERIMENTAL RESULTS AND DISCUSSIONS

A prototype of the proposed circuit configurable bidirectional DC-DC converter with a rated voltage of 150V at TIHB, a rated voltage between 25V and 1050V at TVD, and a rated output power of 1100W is designed for experiments in this paper. Note that the output current is limited to 10A due to the wide voltage range at TVD. The components and parameters used in the designed prototype are listed in TABLE 5. Due to the higher voltages at TVD, SiC-MOSFETs, C2M0025120D with a rated voltage of 1200V manufactured by Wolfspeed [37], are adopted for the switches Q_5, Q_6, Q_7, and Q_8 in this paper. The prototype converter, controlled by the TMS320F28335 from Texas Instruments [38], is shown in Figure 10. Figure 11 shows the recommended control scheme for the proposed converter from TIHB to TVD. From Figure 11, it is observed that the cascaded-buck-boost mode is used when the voltages at TIHB and TVD are within 10% of the difference. When the

TABLE 5. Circuit components and parameters of the prototype circuit.

Voltage at TIHB (V_{TIHB})	150V
Voltage at TVD (V_{TVD})	25V - 1050V
Switching Frequency (f_S)	25kHz
Inductors (L_1, L_2)	800μH
Capacitors (C_{TIHB}, C_{TVD1}, C_{TVD2})	470μF
Switches (Q_1, Q_2, Q_3, Q_4)	IRF4868
Switches (Q_5, Q_6, Q_7, Q_8)	C2M0025120D

voltage at TVD is less than 90% of the voltage at TIHB voltage, the proposed converter will be operated at single-buck mode. The single-boost mode will be used when the voltage at TVD is greater than 110% but less than 400% of the voltage at TIHB. Finally, the interleaved-boost mode is selected when the voltage at TVD is greater than 400% of the voltage at TIHB. After the mode is determined, the circuit can then be reconfigured according to the switch operation states as listed in TABLE 1 and start to adjust and control the duty cycles of PWMs. The control scheme from TVD to TIHB is the reverse operations as illustrated in Figure 11 and is not shown here. For the designed and implemented prototype circuit from TIHB to TVD, the interleaved-boost mode, single-boost mode, cascaded-buck-boost mode, and single-buck mode are operated at the approximate voltages of 600V∼1050V, 165V∼600V, 135∼165V, and 25V∼135V at TVD, respectively when the rated voltage at TIHB is 150V. On the contrary, the interleaved-buck mode, single-buck mode, cascaded-buck-boost mode, and single-boost mode are operated at the approximate voltages of 600V∼1050V, 165V∼600V, 135∼165V, and 25V∼135V at TVD, respectively from TVD to TIHB. Since the voltage at TVD is designed to be between 25V and 1050V, the proposed converter can be used for most retired batteries where their voltages are commonly between 24V and 800V as shown in Figure 1.

Many experiments under the different modes, voltages at TVD, and current conditions have been conducted; however, only the limited experimental results about the interleaved-boost mode, cascaded buck-boost mode, and single-buck mode from TIHB to TVD are shown due to the space. Figure 12 illustrates the experimental waveforms of interleaved-boost mode with the voltages of 150 V and 1050 V at TIHB and TVD, respectively, and the output power of about 1100W at TVD. It can be observed from Figure 12(a), the PWM signals of V_{gs5} and V_{gs8} are complementary and the switching frequency is 25kHz. The drain-source voltages of V_{ds5} and V_{ds8}, indicating the voltage stresses for switches Q_5 and Q_8, are about 1.151kV and 603V, respectively. Figure 12(b) indicates that the current ripples of I_{L1} and I_{L2} are about 7.3A and 7.0A, respectively and the input current ripple can be reduced due to the interleaved mode.

Figure 13 shows the experimental waveforms of cascaded-buck-boost mode with the voltages of 150 V and 150 V at TIHB and TVD, respectively and the output power of

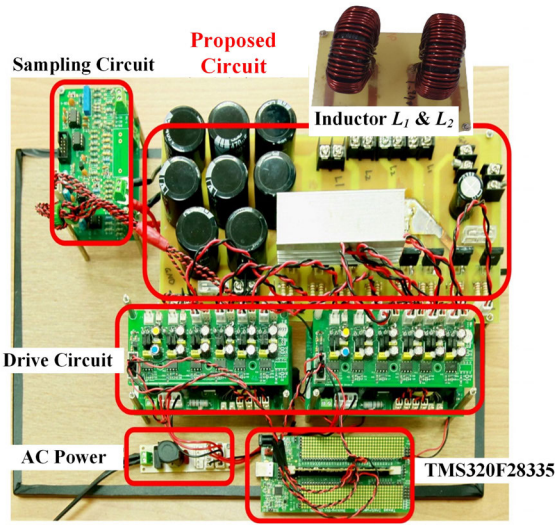

FIGURE 10. Prototype of the proposed converter.

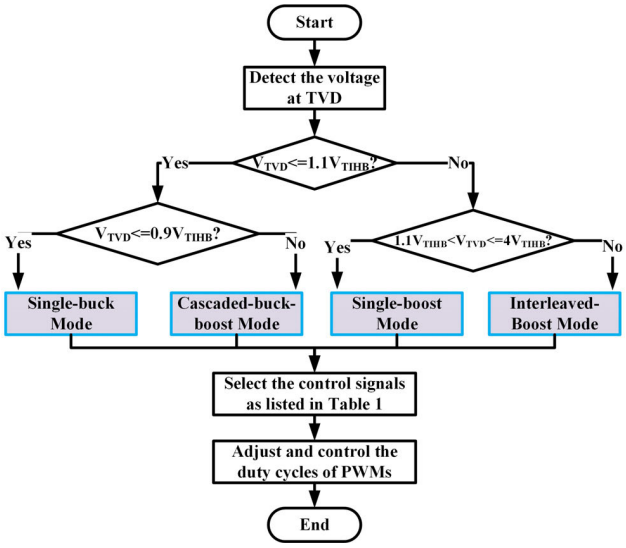

FIGURE 11. Control scheme for a proposed converter from TIHB to TVD.

about 1100W at TIHB. The duty cycle of switch Q_5 is 50 %; therefore, the voltage can be controlled by the duty cycle of switch Q_1. The PWM signals of V_{gs1} and V_{gs2} for the cascaded-buck-boost mode as shown in Figure 13(a) are complementary and the switching frequency is 25kHz. The drain-source voltages of V_{ds1} and V_{ds2}, indicating the voltage stresses for switches Q_1 and Q_2, are about 177 V and 203 V, respectively. Figure 13(b) indicates that the output current at TVD (I_O as denoted) is about 7.5 A. Figure 14 illustrates the experimental waveforms of single-buck mode with the voltages of 150 V and 25 V at TIHB and TVD, respectively and the output power of about 250 W at TVD. Figure 14(a) indicates the PWM signals of V_{gs1} and V_{gs2} are complementary and the duty cycle is about 16.6%. It can also be seen from Figure 14(b) that the output current at TVD (I_O as denoted) is about 10 A. From the above experiments, it

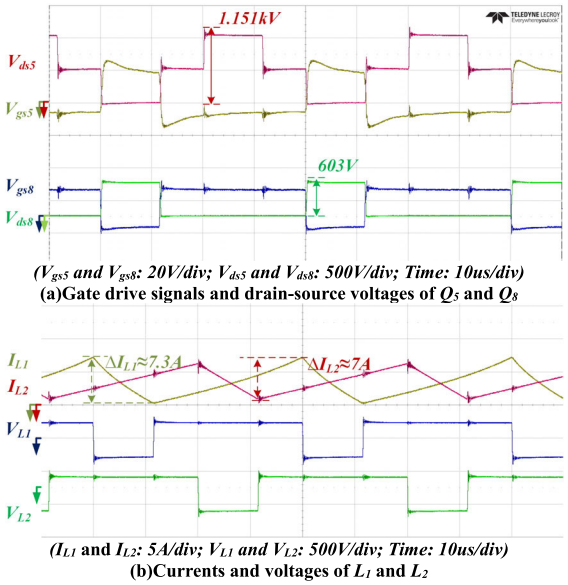

(V_{gs5} and V_{gs8}: 20V/div; V_{ds5} and V_{ds8}: 500V/div; Time: 10us/div)
(a)Gate drive signals and drain-source voltages of Q_5 and Q_8

(I_{L1} and I_{L2}: 5A/div; V_{L1} and V_{L2}: 500V/div; Time: 10us/div)
(b)Currents and voltages of L_1 and L_2

FIGURE 12. Experimental waveforms of interleaved-boost mode for 1050V at TVD.

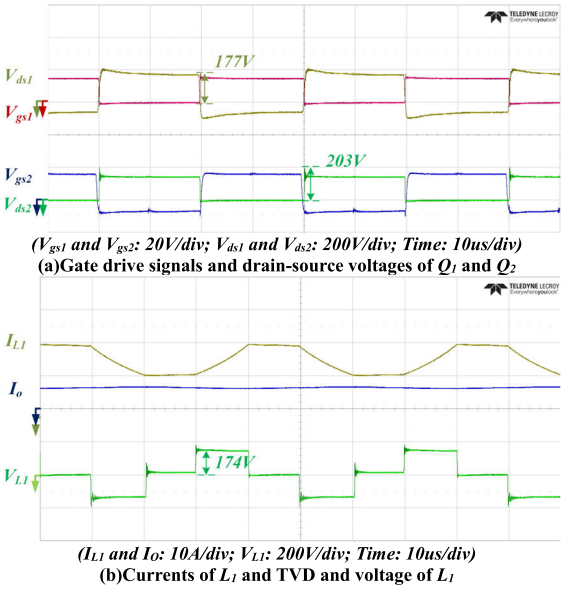

(V_{gs1} and V_{gs2}: 20V/div; V_{ds1} and V_{ds2}: 200V/div; Time: 10us/div)
(a)Gate drive signals and drain-source voltages of Q_1 and Q_2

(I_{L1} and I_O: 10A/div; V_{L1}: 200V/div; Time: 10us/div)
(b)Currents of L_1 and TVD and voltage of L_1

FIGURE 13. Experimental waveforms of cascaded-buck-boost mode for 150V at TVD.

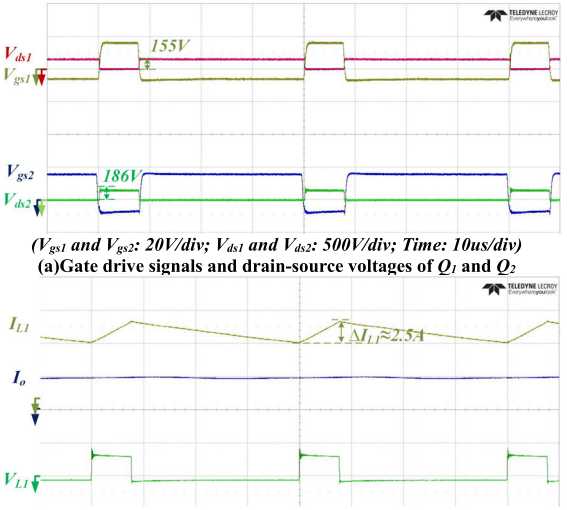

(V_{gs1} and V_{gs2}: 20V/div; V_{ds1} and V_{ds2}: 500V/div; Time: 10us/div)
(a)Gate drive signals and drain-source voltages of Q_1 and Q_2

(I_{L1}: 5A/div; I_O: 10A/div; V_{L1}: 200V/div; Time: 10us/div)
(b) Currents of L_1 and TVD and voltage of L_1

FIGURE 14. Experimental waveforms of single-buck mode for 25V at TVD.

can be verified that the proposed circuit configurable bidirectional DC-DC converter has a wide-range voltage conversion ratio.

Figure 15 shows the conversion efficiencies of the proposed converter operated at the rated input power of 1100W for interleaved-boost mode, single-boost mode, and cascaded-buck-boost mode and at a maximum output current of 10A for single buck mode from the TIHB to TVD. In Figure 15, V_{dc1}, I_{dc1} and P_1 are the voltage, current, and power at TIHB, respectively; V_{dc2}, I_{dc2} and P_2 are the voltage, current, and power at TVD, respectively; and η_1 is the conversion efficiency. From Figure 15, it can be seen that the conversion efficiencies of 97.55%, 97.93%, 94.99%, and 88.20% can be achieved at the voltages about 1050V, 600V, 150V, and 25V for the interleaved-boost mode, single-boost mode, cascaded-buck-boost mode, and single-buck mode, respectively. Figure 16 illustrates the conversion efficiencies of the proposed converter operated at the rated output power of 1100W for interleaved-buck mode, single-buck mode, and cascaded-buck-boost mode and a maximum output current of 10A for single boost mode from the TVD to TIHB. From Figure 16, it can be observed that the conversion efficiencies of 96.66%, 96.94%, 93.60%, and 86.69% can be achieved at the voltages about 1050V, 600V, 150V, and 25V for the interleaved-buck mode, single-buck mode, cascaded-buck-boost mode, and single-boost mode, respectively.

Figure 17 shows the conversion efficiencies of the proposed converter when power is transmitted from TIHB to TVD with the increment of 50V and the constant current of 1A at TVD. From Figure 17, it can be seen that the wide-range voltage conversion, from 25V to 1050V, can be realized and the maximum conversion efficiency is above 98% with the overall approximate conversion efficiencies between 91% and 98%. Figure 18 shows the conversion efficiencies of the proposed converter when power is transmitted from TVD to TIHB with the increment of 50V and the constant current of 1A at TIHB. From Figure 18, it can be seen that the wide-range voltage conversion, from 25V to 1050V, can also be achieved and the maximum conversion efficiency is above 98% with the overall approximate conversion efficiencies between 88% and 98%. Note that when the voltage at TVD is high and the current at TIHB is 1 A, the circuit is operated at the light-load conditions and therefore has lower conversion efficiency from TVD to TIHB. There are two main reasons for the lower efficiency of cascade-buck-boost mode. The first is that the voltage levels at TIHB and TVD are quite

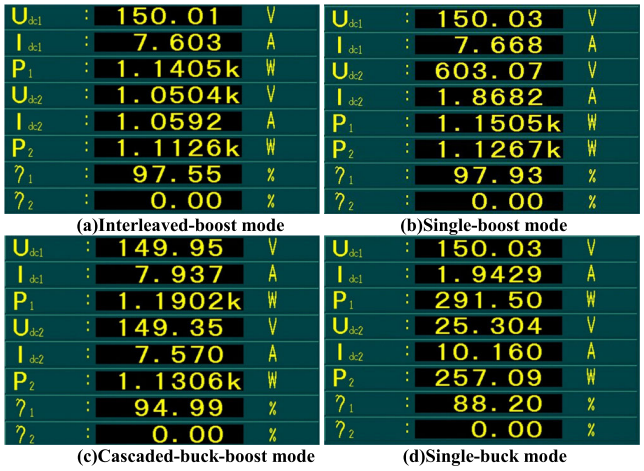

FIGURE 15. Conversion efficiencies of the proposed converter from TIHB to TVD.

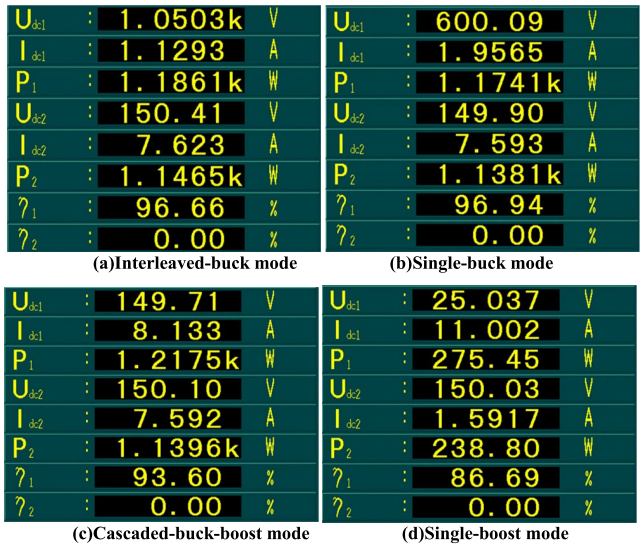

FIGURE 16. Conversion efficiencies of the proposed converter from TVD to TIHB.

close, i.e. the conversion ratio is close to 1, so the conversion efficiency may be lower. The second is more switches operated at the high-frequency switching, which will cause more switching losses. From the experimental results as shown above, the performances of the proposed circuit configurable bidirectional DC-DC converter with a wide-range voltage conversion ratio and bidirectional buck and boost abilities can be demonstrated. Although the proposed converter has significant advantages, the proposed converter requires more switches. Therefore, a detailed cost-benefit analysis under different retired battery scenarios will be conducted in future studies.

It can be seen from Figure 1 that the voltage level ranges of retired batteries may be varied from 24V for electric scooters to 800V for electric trucks. Due to the wide-range voltage conversion ratio and bidirectional buck and boost abilities as validated in the above experimental results, the proposed

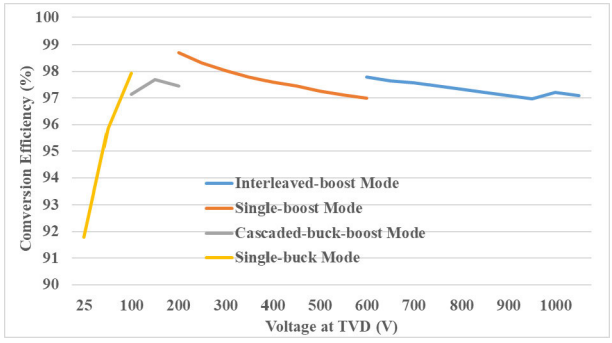

FIGURE 17. Conversion efficiencies of the proposed converter from TIHB to TVD with an output current of 1A at TVD.

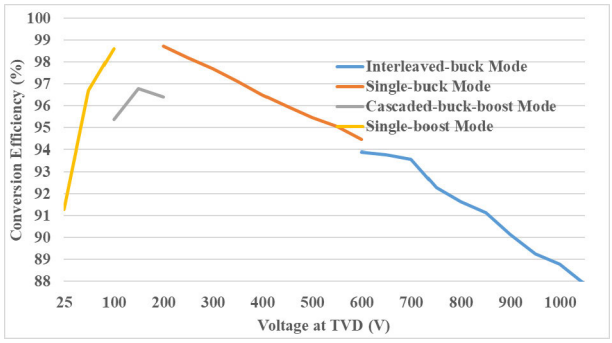

FIGURE 18. Conversion efficiencies of the proposed converter from TVD to TIHB with an output current of 1A at TIHB.

circuit configurable bidirectional DC-DC converter can be used for energy conversion of retired batteries with different voltage levels. As an example for actual applications, the retired batteries can be connected to the TIHB of the proposed converter and then the output voltage at TVD can be set to 150-200 V and be used for a DC grid. It is also possible to use a bidirectional inverter with a rated voltage of 150-200V at the DC terminal and a rated voltage of 110V/60Hz at the AC terminal to interconnect to power grids. The above voltages can be adjusted according to different usage scenarios; however, the circuit topology and control schemes proposed in this paper don't need to modify. The proposed converter can also be used in healthy batteries without additional challenges. Most of the healthy batteries used in EVs will be equipped with dedicated bidirectional converters in a specific voltage conversion ratio; therefore, they may not need a converter with the bidirectional buck and boost abilities. However, if a dedicated bidirectional converter is required for a retired battery, it will cause resource waste and increase the difficulty of reuse. Due to the configurable structure design and control, the proposed converter is particularly suitable for the energy conversion of different retired batteries.

V. CONCLUSION

The retired batteries have diverse voltage levels; therefore, a bidirectional DC-DC converter with a wide-range voltage

conversion ratio and bidirectional voltage boost and buck abilities to change the various voltage levels of retired batteries for different application scenarios is vital. A circuit configurable bidirectional DC-DC converter for retired batteries was proposed in this paper. The proposed converter was constituted by cascading a two-phase interleaved half-bridge circuit and a voltage-doubler circuit. The proposed converter can be operated in the interleaved boost/buck mode, single boost/buck mode, cascaded-buck-boost mode, or single buck/boost mode concerning the voltage levels at different terminals of the proposed converter. Due to the configurable structure design and control of the proposed converter, a wide-range voltage conversion ratio and bidirectional buck and boost abilities can be achieved. A prototype circuit for the proposed bidirectional DC-DC converter with a rated voltage of 150V at TIHB, a rated voltage between 25V and 1050V at TVD, and a rated power of 1100W was designed and realized. Experimental results showed that the proposed converter can be configured into the diverse operating modes for different voltage levels of retired batteries and the maximum conversion efficiency of above 98% can be realized. Although the recommended control scheme for the proposed converter was provided, it is still worthy of further research and optimization. Besides, the proposed converter can also be extended. The expansion of the proposed converter including more series or parallel TIHBs and TVDs will be investigated in the future.

REFERENCES

[1] S. A. Gorji, H. G. Sahebi, M. Ektesabi, and A. B. Rad, "Topologies and control schemes of bidirectional DC–DC power converters: An overview," *IEEE Access*, vol. 7, pp. 117997–118019, 2019.

[2] M. Forouzesh, Y. P. Siwakoti, S. A. Gorji, F. Blaabjerg, and B. Lehman, "Step-up DC–DC converters: A comprehensive review of voltage-boosting techniques, topologies, and applications," *IEEE Trans. Power Electron.*, vol. 32, no. 12, pp. 9143–9178, Dec. 2017.

[3] K. Tytelmaier, O. Husev, O. Veligorskyi, and R. Yershov, "A review of non-isolated bidirectional DC–DC converters for energy storage systems," in *Proc. YSF*, Kharkiv, Ukraine, 2016, pp. 22–28.

[4] B. Mangu, S. Akshatha, D. Suryanarayana, and B. G. Fernandes, "Grid-connected PV-wind-battery-based multi-input transformer-coupled bidirectional DC–DC converter for household applications," *IEEE J. Emerg. Sel. Topics Power Electron.*, vol. 4, no. 3, pp. 1086–1095, Sep. 2016.

[5] Y. Du, X. Zhou, S. Bai, S. Lukic, and A. Huang, "Review of non-isolated bi-directional DC–DC converters for plug-in hybrid electric vehicle charge station application at municipal parking decks," in *Proc. 25th Annu. IEEE Appl. Power Electron. Conf. Expo. (APEC)*, Palm Springs, CA, USA, Feb. 2010, pp. 1145–1151.

[6] O. C. Onar, J. Kobayashi, D. C. Erb, and A. Khaligh, "A bidirectional high-power-quality grid interface with a novel bidirectional noninverted buck–boost converter for PHEVs," *IEEE Trans. Veh. Technol.*, vol. 61, no. 5, pp. 2018–2032, Jun. 2012.

[7] C.-M. Lai, Y.-C. Lin, and D. Lee, "Study and implementation of a two-phase interleaved bidirectional DC/DC converter for vehicle and DC-microgrid systems," *Energies*, vol. 8, no. 9, pp. 9969–9991, Sep. 2015.

[8] R. Kumar. (May 2021). *Electric Vehicle Market*. [Online]. Available: https://www.alliedmarketresearch.com/electric-vehicle-market

[9] M. Rehme, S. Richter, A. Temmler, and U. Götze, "Second-life battery applications: Market potentials and contribution to the cost effectiveness of electric vehicles," in *Proc. CoFAT*, 2016, pp. 1–8.

[10] Y. Zhao, O. Pohl, A. I. Bhatt, G. E. Collis, P. J. Mahon, T. Rüther, and A. F. Hollenkamp, "A review on battery market trends, second-life reuse, and recycling," *Sustain. Chem.*, vol. 2, no. 1, pp. 167–205, Mar. 2021.

[11] (May 2021). *Second-Life Electric Vehicle Batteries 2020–2030*. [Online]. Available: https://www.idtechex.com/tw/research-report/second-life-electric-vehicle-batteries-2020-2030/681

[12] *Voltage Classes for Electric Mobility*, ZVEI-German Electrical and Electronic Manufacturers' Association, Frankfurt, Germany, Dec. 2013.

[13] H. Matsuo and F. Kurokawa, "New solar cell power supply system using a boost type bidirectional DC–DC converter," *IEEE Trans. Ind. Electron.*, vol. IE-31, no. 1, pp. 51–55, Feb. 1984.

[14] F. Caricchi, F. Crescimbini, G. Noia, and D. Pirolo, "Experimental study of a bidirectional DC–DC converter for the DC link voltage control and the regenerative braking in PM motor drives devoted to electrical vehicles," in *Proc. IEEE ASPEC*, Orlando, FL, USA, Feb. 1994, pp. 381–386.

[15] J. Majo, L. Martinez, A. Poveda, L. G. de Vicuna, F. Guinjoan, F. Sanchez, M. Valentin, and J. C. Marpinard, "Large-signal feedback control of a bidirectional coupled-inductor Cuk converter," *IEEE Trans. Ind. Electron.*, vol. 39, no. 5, pp. 429–436, Oct. 1992.

[16] M.-S. Song, Y.-D. Son, and K.-H. Lee, "Non-isolated bidirectional soft-switching SEPIC/ZETA converter with reduced ripple currents," *J. Power Electron.*, vol. 14, no. 4, pp. 649–660, Jul. 2014.

[17] S. Waffler and J. W. Kolar, "A novel low-loss modulation strategy for high-power bidirectional buck + boost converters," *IEEE Trans. Power Electron.*, vol. 24, no. 6, pp. 1589–1599, Jun. 2009.

[18] H. S. Chung, A. Ioinovici, and W.-L. Cheung, "Generalized structure of bi-directional switched-capacitor DC/DC converters," *IEEE Trans. Circuits Syst. I, Fundam. Theory Appl.*, vol. 50, no. 6, pp. 743–753, Jun. 2003.

[19] O. Garcia, P. Zumel, A. de Castro, and J. A. Cobos, "Automotive DC–DC bidirectional converter made with many interleaved buck stages," *IEEE Trans. Power Electron.*, vol. 21, no. 3, pp. 578–586, May 2006.

[20] F. Z. Peng, F. Zhang, and Z. Qian, "A magnetic-less DC–DC converter for dual voltage automotive systems," in *Proc. IEEE IAS*, Pittsburgh, PA, USA, Oct. 2002, pp. 1303–1310.

[21] M. K. Kazimierczuk, D. Q. Vuong, B. T. Nguyen, and J. A. Weimer, "Topologies of bidirectional PWM DC–DC power converters," in *Proc. IEEE NAECON*, Dayton, OH, USA, May 1993, pp. 435–441.

[22] A. A. Aboulnaga and A. Emadi, "Performance evaluation of the isolated bidirectional Cuk converter with integrated magnetics," in *Proc. IEEE APEC*, Aachen, Germany, vol. 2, Feb. 2004, pp. 1557–1562.

[23] A. Ruseler and I. Barbi, "Isolated Zeta-SEPIC bidirectional DC–DC converter with active-clamping," in *Proc. Brazilian Power Electron. Conf.*, Gramado, Brazil, Oct. 2013, pp. 123–128.

[24] M. Kwon, J. Park, and S. Choi, "A bidirectional three-phase push–pull converter with dual asymmetrical PWM method," *IEEE Trans. Power Electron.*, vol. 31, no. 3, pp. 1887–1895, Mar. 2016.

[25] M. Khodabakhshian, E. Adib, and H. Farzanehfard, "Forward-type resonant bidirectional DC–DC converter," *IET Power Electron.*, vol. 9, no. 8, pp. 1753–1760, 2016.

[26] B. Zhao, Q. Song, W. Liu, and Y. Sun, "Overview of dual-active-bridge isolated bidirectional DC–DC converter for high-frequency-link power-conversion system," *IEEE Trans. Power Electron.*, vol. 29, no. 8, pp. 4091–4106, Aug. 2014.

[27] P. He and A. Khaligh, "Comprehensive analyses and comparison of 1 kw isolated DC–DC converters for bidirectional EV charging systems," *IEEE Trans. Transport. Electrific.*, vol. 3, no. 1, pp. 147–156, Mar. 2017.

[28] H. Tao, A. Kotsopoulos, J. L. Duarte, and M. A. M. Hendrix, "Family of multiport bidirectional DC–DC converters," *IEE Proc.-Electr. Power Appl.*, vol. 153, no. 3, pp. 451–458, May 2006.

[29] N. Elsayad, H. Moradisizkoohi, and O. A. Mohammed, "Design and implementation of a new transformerless bidirectional DC–DC converter with wide conversion ratios," *IEEE Trans. Ind. Electron.*, vol. 66, no. 9, pp. 7067–7077, Sep. 2019.

[30] Y. Zhang, W. Zhang, F. Gao, S. Gao, and D. J. Rogers, "A switched-capacitor interleaved bidirectional converter with wide voltage-gain range for super capacitors in EVs," *IEEE Trans. Power Electron.*, vol. 35, no. 2, pp. 1536–1547, Feb. 2020.

[31] M. P. Hirth, R. Gules, and C. H. Illa Font, "A wide conversion ratio bidirectional modified SEPIC converter with nondissipative current snubber," *IEEE J. Emerg. Sel. Topics Power Electron.*, vol. 9, no. 2, pp. 1350–1360, Apr. 2021.

[32] S. M. Fardahar and M. Sabahi, "New expandable switched capacitor/switched-inductor high-voltage conversion ratio bidirectional DC–DC converter," *IEEE Trans. Power Electron.*, vol. 35, no. 3, pp. 2480–2487, Mar. 2020.

[33] N. Elsayad, H. Moradisizkoohi, and O. A. Mohammed, "A new hybrid structure of a bidirectional DC–DC converter with high conversion ratios for electric vehicles," *IEEE Trans. Veh. Technol.*, vol. 69, no. 1, pp. 194–206, Jan. 2020.
[34] G. P. Muralidharan and K. Bhaskar, "High step-down conversion ratio interleaved DC–DC converter," in *Proc. IEEE ICECCT*, Coimbatore, India, Mar. 2015, pp. 1–4.
[35] C. F. Chuang, C. T. Pan, and H. C. Cheng, "A novel transformerless interleaved four-phase step-down DC converter with low switch voltage stress and automatic uniform current-sharing characteristics," *IEEE Trans. Power Electron.*, vol. 26, no. 1, pp. 406–417, Jan. 2016.
[36] J. Teng, S. Chen, S. Luan, and J. Xu, "Bidirectional DC–DC converter with a wide-range voltage conversion ratio," in *Proc. IEEE 4th Int. Future Energy Electron. Conf. (IFEEC)*, Nov. 2019, pp. 1–6.
[37] Wolfspeed. (May 2021). *C2M0025120D User Manual*. [Online]. Available: https://www.wolfspeed.com/medi.a/downloads/161/C2M0025120D.pdf
[38] Texas Instruments. (May 2021). *TI TMS320F28335 Data Manual*. [Online]. Available: http://www.ti.com/lit/ds/symlink/

JENHAO TENG (Senior Member, IEEE) received the B.S., M.S., and Ph.D. degrees in electrical engineering from National Sun Yat-sen University, Kaohsiung, Taiwan, in 1991, 1993, and 1996, respectively.

From 1998 to 2010, he was with I-Shou University, Kaohsiung. Since 2011, he has been with National Sun Yat-sen University, where he is currently a Professor with the Department of Electrical Engineering. His current research interests include smart grid, design and analysis of green and renewable energy, conversion efficiency enhancement of power converters, and utilization of heuristic techniques in power engineering.

POSHENG SHEN is currently pursuing the Ph.D. degree with the Department of Electrical Engineering, National Sun Yat-sen University, Kaohsiung, Taiwan. His research interests include conversion efficiency enhancement of power converters and industrial automation.

BOHSIEN LIU is currently pursuing the M.S. degree with the Department of Electrical Engineering, National Sun Yat-sen University, Kaohsiung, Taiwan. His research interest includes bidirectional power converter design.

SIWEI CHEN received the M.S. degree in electrical engineering from National Sun Yat-sen University, Kaohsiung, Taiwan. His research interest includes fully digitalized control for power converters.